Single siRNA Nanocapsules for Effective siRNA Brain Delivery and Glioblastoma Treatment

Yan Zou, Xinhong Sun, Yibin Wang, Chengnan Yan, Yanjie Liu, Jia Li, Dongya Zhang, Meng Zheng,* Roger S. Chung, and Bingyang Shi*

Small interfering RNA (siRNA) has been considered as a highly promising therapeutic agent for human cancer treatment including glioblastoma (GBM), which is a fatal disease without effective therapy methods. However, siRNA-based GBM therapy is seriously hampered by a number of challenges in siRNA brain delivery including poor stability, short blood circulation, low blood–brain barrier (BBB) penetration, and tumor accumulation, as well as inefficient siRNA intracellular release. Herein, an Angiopep-2 (Ang) functionalized intracellular-environment-responsive siRNA nanocapsule (Ang-NC$_{ss}$(siRNA)) is successfully developed as a safe and efficient RNAi agent to boost siRNA-based GBM therapy. The experimental results demonstrate that the developed Ang-NC$_{ss}$(siRNA) displays long circulation in plasma, efficient BBB penetration capability, and GBM accumulation and retention, as well as responsive intracellular siRNA release due to the unique design of small size (25 nm) with polymeric shell for siRNA protection, Ang functionalization for BBB crossing and GBM targeting, and disulfide bond as a linker for intracellular-environment-responsive siRNA release. Such superior properties of Ang-NC$_{ss}$(siRNA) result in outstanding growth inhibition of orthotopic U87MG xenografts without causing adverse effects, achieving remarkably improved survival benefits. The developed siRNA nanocapsules provide a new strategy for RNAi therapy of GBM and beyond.

Glioblastoma (GBM), an invasive human intracranial malignancy with high mortality and morbidity, remains incurable to date.[1] Enormous efforts and research have been devoted to treat GBM in the last decades.[2] The clinical standard care for GBM patients is maximal surgical resection followed by chemo- and radiation therapy.[3] Nevertheless, the median overall survival after multimodal treatment has not been extended beyond 15 months.[4] Increasing evidences prove that the complex and heterogeneity of GBM underlies the ineffectiveness of current therapeutics.

RNA interference (RNAi) with a high specifically and low toxicity has been considered as a highly promising modality for treating various intractable GBM.[5] However, the lack of siRNA vectors remains a key obstacle for the application of RNAi technology in disease therapy.[6] Viruses have shown excellent siRNA delivery capability, however, the mutagenic toxicity and immunogenicity seriously hinder their clinical applications.[7] Comparatively, nonviral vectors such as cationic liposomes,[8] polymeric,[9] and inorganic nanoparticles[10] are able to deliver siRNA, but they still face efficiency and safety issues. Remarkably, most nonviral delivery nanocarriers were cationic or lipid based materials that have excessive positive surface charge, which normally induce systemic toxicity and low selectively in vivo.[11] Furthermore, poor blood stability, the existence of blood–brain barrier (BBB), off-target issues, as well as inefficient controlled release are tough barriers for the RNAi therapy of GBM.[12] Therefore, seeking new siRNA delivery strategy is highly desired, but very challenging.

To address the aforementioned challenges, a multifunctional single siRNA nanocapsule has been developed to maximize systemic siRNA brain delivery for GBM RNAi therapy for the first time. siRNA molecules are cross-linked via disulfide bonds (SS) to form a self-encapsulating polymerization shell to protect siRNA from degradation and provide a novel multistep delivery process whereby intracellular siRNA release is triggered in the presence of abundant glutathione (GSH) in the cytoplasm. Inspired by the fact that both BBB endothelial cells and GBM tissue highly expressed a receptor-related protein 1 (LRP-1), a specific LRP-1 ligand Angiopep-2 is conjugated on the surface of developed siRNA capsules for facilitating BBB permeation and GBM tissue targeting.[13] Importantly, the realization of small size of siRNA nanocapsule and nearly 100% siRNA encapsulation by this novel self-encapsulation strategy lead to highly effective siRNA BBB penetration and GBM RNAi

Dr. Y. Zou, X. Sun, Y. Wang, C. Yan, Y. Liu, D. Zhang, Prof. M. Zheng, Prof. B. Shi
Henan-Macquarie University Joint Centre for Biomedical Innovation
School of Life Sciences
Henan University
Kaifeng, Henan 475004, China
E-mail: mzheng@henu.edu.cn; bs@henu.edu.cn
Dr. Y. Zou, Dr. J. Li, Prof. R. S. Chung, Prof. B. Shi
Centre for Motor Neuron Disease Research
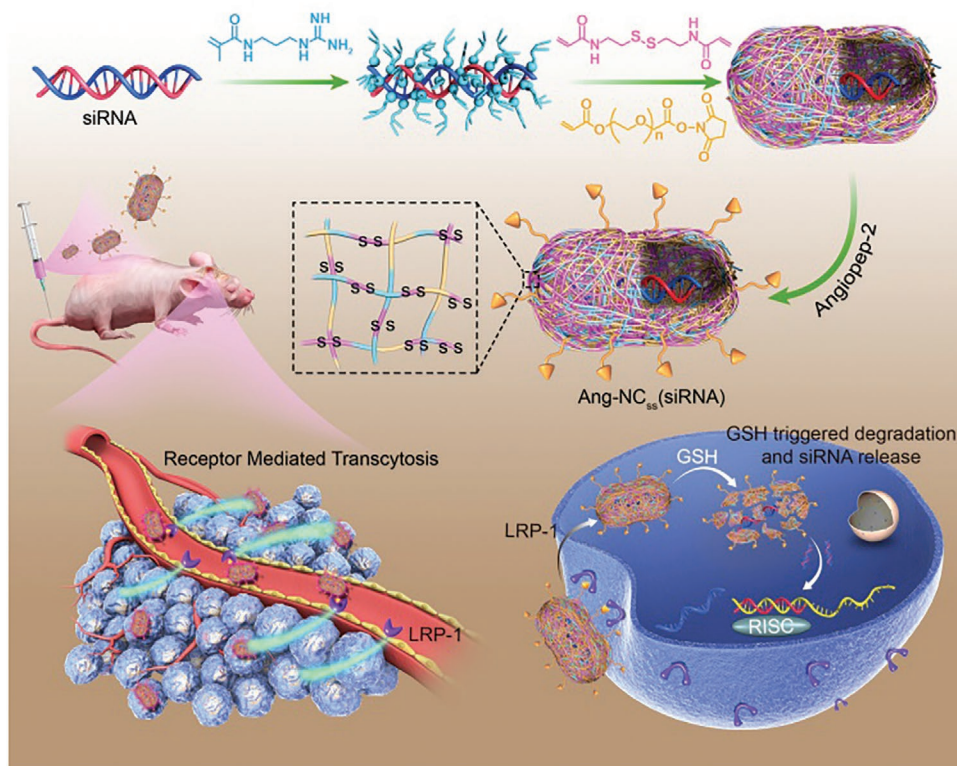Department of Biomedical Sciences
Faculty of Medicine and Health Sciences
Macquarie University
Sydney, NSW 2109, Australia

The ORCID identification number(s) for the author(s) of this article can be found under https://doi.org/10.1002/adma.202000416.

Scheme 1. Illustration of Ang-NC$_{ss}$(siRNA) nanocapsule preparation, efficient BBB penetration, highly specific GBM targeting, responsive drug release, and gene silencing.

therapy. The brain delivery capability and GBM RNAi effect of Ang-NC$_{ss}$(siRNA) nanocapsules have been systematically evaluated in vitro and in vivo, the results demonstrate that it can effectively permeate the BBB, actively internalized by U87MG GBM cells, and responsively release siRNA into the cytoplasm. Moreover, the Ang-NC$_{ss}$(siRNA) nanocapsules can also induce a potent and robust anti-GBM effect and remarkably expand the survival time of mice with an orthotopic human GBM xenograft. The outstanding RNAi and superb safety performances of these brain targeting reduction-responsive siRNA nanocapsules make them appealing for GBM therapy.

Ang-NC$_{ss}$(siRNA) nanocapsules were readily prepared as shown in **Scheme 1**. Briefly, positively charged acrylate guanidine was decorated on the surface of siRNA via electrostatic absorption, followed by polymerized with cross-linkers like *N,N′*-bis(acryloyl) cystamine containing disulfide bonds and neutral molecular polyethylene glycol with acylate and succinate functional end groups. The final Ang-NC$_{ss}$(siRNA) siRNA nanocapsules were obtained by functionalizing siRNA nanocapsules with Angiopep-2 (Ang) peptide via amidation chemical reaction. A nonreduction control (referred to as Ang-NC(siRNA)) was fabricated in the same way with replacing the reduction cross-linker by nondegradable cross-linker *N,N′*-methylene bisacrylamide. Taking the advantage of this interfacial polymerization strategy, no covalent bond is formed between the resulted polymeric shell matrix and encapsulated siRNA payload, which ensures that the siRNA can be released responsively in the intracellular environment due to the existence of 2×10^{-3} to 10×10^{-3} M high-concentration GSH in

the cytoplasm.[14] After polymerization and encapsulation, the nanocapsules were purified using a centrifugal filter to remove the unreacted monomers and unbound Ang molecules.

The average size of Ang-NC$_{ss}$(siRNA) was 25.3 nm with a relatively narrow size distribution (PDI 0.21) and nearly neutral surface charge (Table S1, Supporting Information and **Figure 1**a). Given that naked siRNA had an average diameter of 5 nm, this further confirms the successful preparation of Ang-NC$_{ss}$(siRNA) nanocapsules. The nonreduction Ang-NC(siRNA) and nontarget NC$_{ss}$(siRNA) controls were observed that displayed the similar size. Transmission electron microscopy (TEM) photograph showed that Ang-NC$_{ss}$(siRNA) adopted a spherical morphology in aqueous solution (Figure 1b). Remarkably, a dark core with an average diameter around 5.3 nm in each nanocapsule was observed, which is in consistence with the size of a naked siRNA and reported nanocapsules with single siRNA or protein inside [5d,15] To investigate the stability of the Ang-NC$_{ss}$(siRNA), nanocapsules and naked siRNA control were incubated in cell culture media containing 10% fetal bovine serum (FBS) for 1 and 12 h, respectively. Agarose gel electrophoresis showed that nanocapsule siRNA maintained excellent integrity at 1 h and even 12 h, while naked siRNA was degraded at 1 h and could not be detected at 12 h (Figure 1c and Figure S1, Supporting Information), indicating that the siRNA payload was not damaged by fabrication procedure and the resulted nanocapsules can efficiently protect the encapsulated siRNA from enzyme degradation. We further investigated the responsive release in vitro by measuring the siRNA release profile in GSH buffer using PBS as control. The results
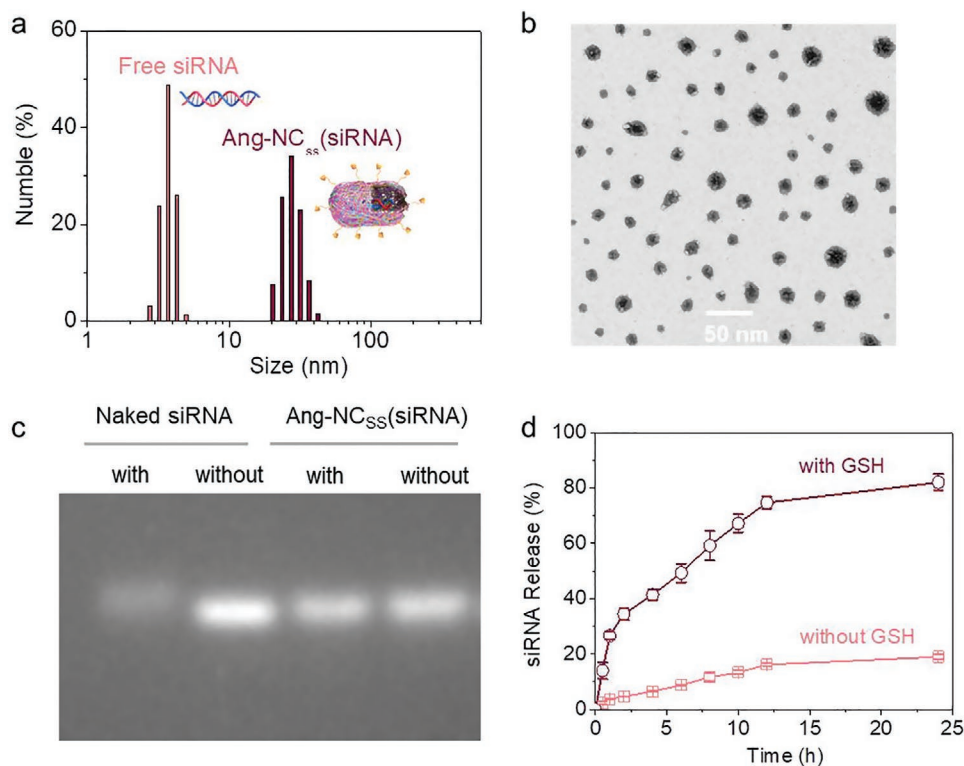
Figure 1. a) Size distribution of Ang-NC$_{ss}$(siRNA) and free siRNA determined by DLS. b) TEM images of Ang-NC$_{ss}$(siRNA). c) Gel retardation assays of Ang-NC$_{ss}$(siRNA) and naked siRNA with or without FBS incubation for 1 h. d) In vitro siRNA release behavior of Ang-NC$_{ss}$(siRNA). The release studies were performed at pH 7.4 and 37 °C either in the presence or absence of 10×10^{-3} M GSH.

revealed that less than 20% siRNA was released in 24 h under physiological conditions in the absence of GSH (Figure 1d). In contrast, nearly 80% loaded siRNA was released within 24 h in the presence of 10×10^{-3} M GSH resulting from fast degradation of the nanocapsule shell. These in vitro results indicate that Ang-NC$_{ss}$(siRNA) may provide a unique solution to simultaneously resolve the low stability and inefficient intracellular release issues in siRNA delivery confronted by conventional siRNA delivery systems.

To evaluate the BBB transcytosis capability of Ang-NC$_{ss}$(siRNA), we established an in vitro BBB model as our previous work.[16] A time-dependent BBB permeation behavior of nanocapsules was observed (**Figure 2**a). The cumulative transport ratio of Ang-NC$_{ss}$(siRNA) was 2.2-fold higher than that of NC$_{ss}$(siRNA), which is mainly ascribed to Ang functionalized nanocapsules that can cross the BBB via an LRP-1 mediated transcytosis mechanism. In addition to brain capillary endothelial cells, LRP-1 is also overexpressed on the membrane of U87 MG human glioblastoma cells.[17] The cellular uptake and intracellular siRNA release of nanocapsules with U87MG cells were investigated with flow cytometry and confocal laser scanning microscopy (CLSM), respectively. Figure 2b and Figure S2a (Supporting Information) demonstrated that Cy5-labeled Ang-NC$_{ss}$(siRNA) had the best cellular uptake in U87MG cells, which was 3.5- and 1.9-fold higher than that of Ang-NC(siRNA) and NC$_{ss}$(siRNA), respectively. Interestingly, pretreating U87MG cells with free Ang induced a pronounced reduction of cellular uptake for Ang-NC$_{ss}$(siRNA), corroborating that these

nanocapsules present active targeting ability to U87MG cells. CLSM results revealed that U87MG cells incubated with Ang-NC$_{ss}$(siRNA) exhibited strong cytoplasmic fluorescence and could escape from the endosome at 4 h, confirming the efficient cellular uptake and responsive intracellular siRNA release of the developed Ang-NC$_{ss}$(siRNA). It should be noted that the abundant guanidine group can help the siRNA nanocapsules penetrate the endosomal membrane for efficient endosome escape and transport of siRNA nanocapsules into cytoplasm.[18] In contrast, nontargeted NC$_{ss}$(siRNA) and nonreduction Ang-NC(siRNA) treated cells had obviously less fluorescence and there was almost no fluorescence detected in naked siRNA incubated cells (Figure 2c and Figure S2b, Supporting Information). The experimental results suggest that Ang-NC$_{ss}$(siRNA) is able to efficiently target U87MG cells via the active endocytosis with the help of Ang and also responsively release the siRNA payload into the cytoplasm triggered by GSH in the intracellular environment.

3-(4,5-Dimethylthiazol-2-yl)-2,5-diphenyltetrazolium bromide (MTT) assays showed that siRNA nanocapsules including Ang-NC$_{ss}$(siRNA), NC$_{ss}$(siRNA), and Ang-NC(siRNA), either at the concentration of 200 or 400×10^{-9} M, were nontoxic to U87MG cells, signifying their good biocompatibility (Figure 2d). To evaluate the gene silencing efficacy of Ang-NC$_{ss}$(siRNA), transfection studies were performed using luciferase siRNA (siGL3) and U87MG cells stably expressing luciferase (U87MG-luc). Cells treated with Ang-NC$_{ss}$(siGL3) displayed 67% down-regulation in the luciferase expression at siRNA concentration of 400×10^{-9} M

**ADVANCED
SCIENCE NEWS**

www.advancedsciencenews.com

**ADVANCED
MATERIALS**

www.advmat.de
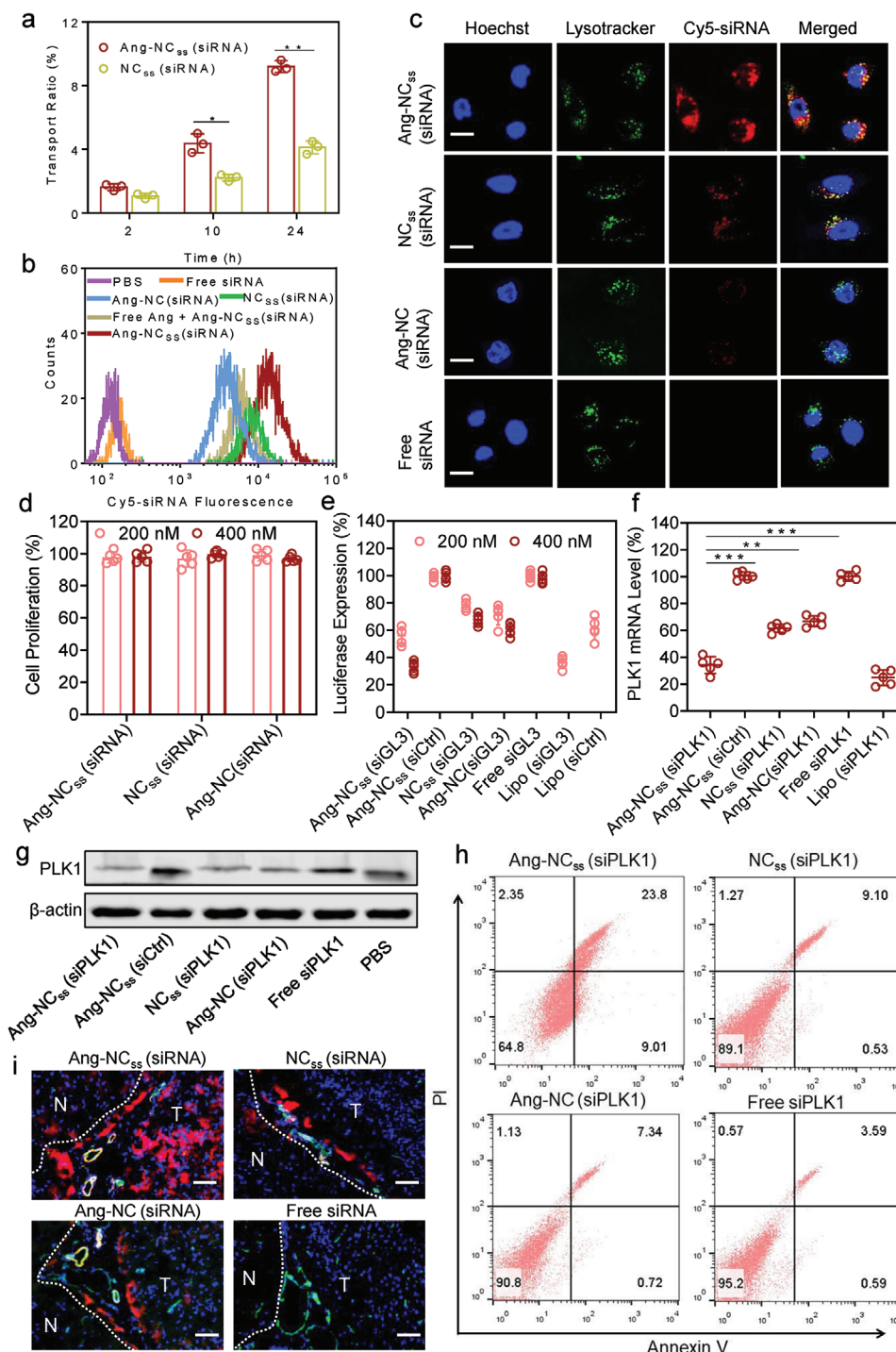
Figure 2. a) Cumulative transport ratio of Ang-NC$_{ss}$(siRNA), NC$_{ss}$(siRNA), and Ang-NC(siRNA) nanocapsules across the in vitro BBB barrier at 2, 10, and 24 h (Cy5-siRNA concentration: 200×10^{-9} M). Data are presented as mean ± SD ($n = 3$, one-way analysis of variance (ANOVA) and Tukey multiple comparisons tests, $*p < 0.05$, $**p < 0.01$). b) Cellular uptake of U87MG cells in the substrate chamber of the BBB model treated with Ang-NC$_{ss}$(siRNA), NC$_{ss}$(siRNA), Ang-NC(siRNA), and free siRNA for 24 h incubation and studied by flow cytometry. The competitive inhibition experiments were performed by pretreating U87MG cells with free Ang ($200 \mu g \ mL^{-1}$) for 4 h before adding Ang-NC$_{ss}$(siRNA). c) CLSM images of U87MG cells following transfection with Ang-NC$_{ss}$(siRNA) (Cy5-siRNA dosage: 200×10^{-9} M) for 4 h. For each panel, the images from left to right were cell nuclei stained by Hochest (blue), lysosome stained by lysotracker green (green), Cy5-siRNA (red), and overlays of the three images. The bar represents 20 µm. d) Cell viability of U87MG glioblastoma cells following 48 h incubation with Ang-NC$_{ss}$(siRNA), NC$_{ss}$ (siRNA), and Ang-NC(siRNA). e) In vitro luciferase gene knockdown efficacy of Ang-NC$_{ss}$(siGL3), Ang-NC$_{ss}$(siCtrl), NC$_{ss}$(siGL3), Ang-NC(siGL3), free siGL3, Lipo (siGL3), and Lipo (siCtrl) in U87MG cells. The transfection was carried out for 48 h. f) PLK1 mRNA level of Ang-NC$_{ss}$(siPLK1) in U87MG cells following 48 h incubation (400×10^{-9} M siPLK1 or siCtrl). Lipo (siPLK1) was used as a positive control. Data are presented as mean ± SD ($n = 5$, one-way Anova and Tukey multiple comparisons tests,

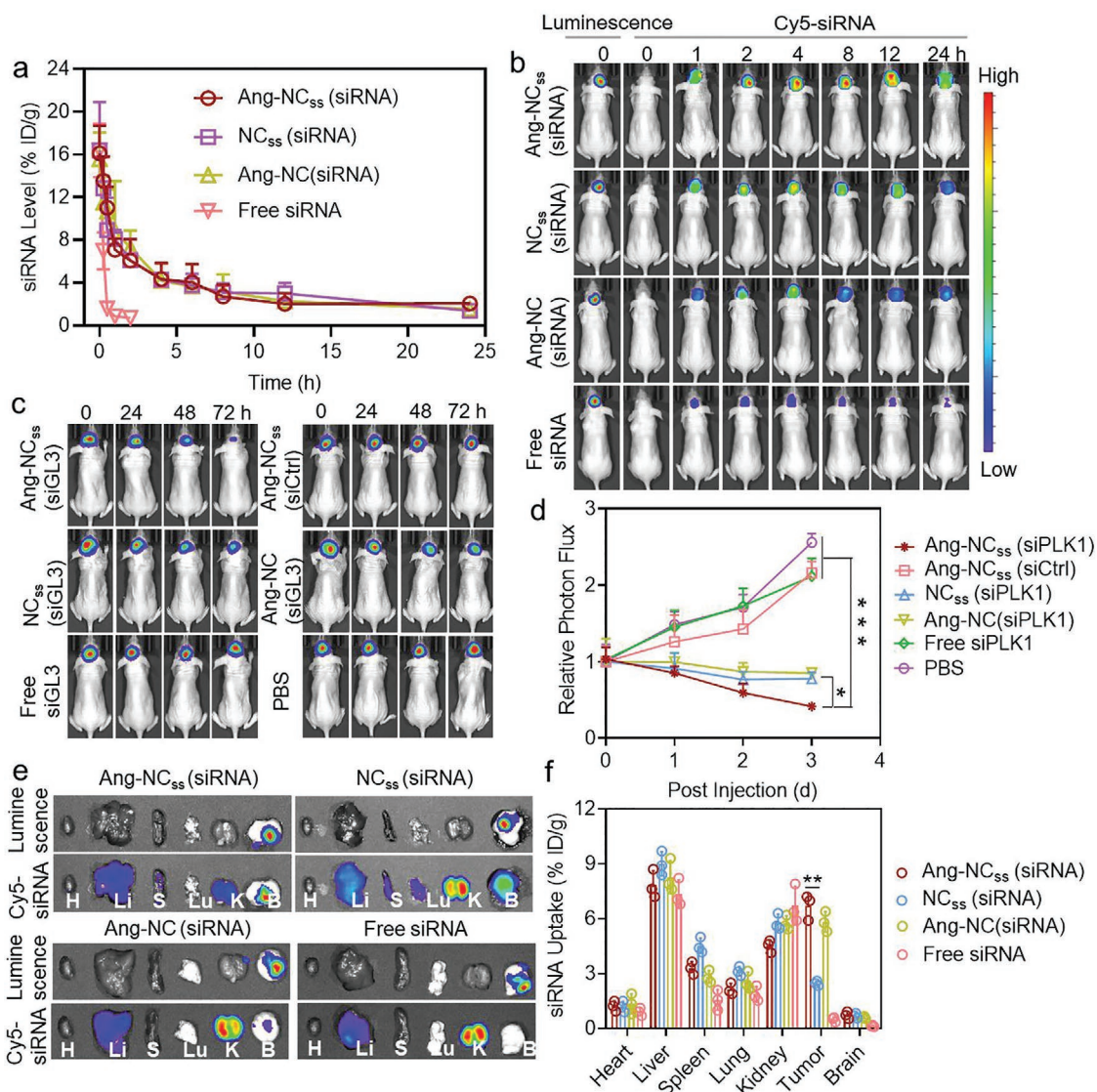(Figure 2e). Meanwhile, cells treated with scrambled control nanocapsules Ang-NC$_{ss}$(siCtrl) did not show downregulation. Moreover, NC$_{ss}$(siRNA) and Ang-NC(siRNA) induced significantly lower knocking down efficiencies in the luciferase expression, which were 33% and 39%, respectively. We then carried out quantitative real-time experiment with U87MG cells transfected with Polo like kinase 1 specific siRNA (siPLK1) nanocapsules. Figure 2f shows that the relative PLK1 mRNA expression of cells treated with Ang-NC$_{ss}$(siPLK1) (34%) was significantly lower than those with NC$_{ss}$(siPLK1) and Ang-NC (siPLK1) (61% and 67%, respectively). As expected, Ang-NC$_{ss}$(siCtrl) and free siPLK1 did not cause any reduction of PLK1 mRNA level. Interestingly, Ang-NC$_{ss}$(siRNA) displayed comparable gene knockdown capability but less toxic in contrast with a commercial positive control (lipofectamine 2000). Western blot assays further confirmed that U87MG cells treated with Ang-NC$_{ss}$(siPLK1) had remarkably low PLK1 protein level (Figure 2g and Figure S3, Supporting Information). To further unveil the gene silencing activity of Ang-NC$_{ss}$(siRNA), apoptosis studies using Annexin V and PI double staining showed that Ang-NC$_{ss}$(siPLK1) induced significantly apoptosis (≈32.8%) of U87MG cells, which was more potent than NC$_{ss}$(siPLK1) (≈9.5%) and Ang-NC(siPLK1) (≈8.1%) controls Almost no cell apoptosis was observed for free siPLK1. The superior gene knockdown efficacy of Ang-NC$_{ss}$(siPLK1) nanocapsules results from the efficient U87MG cell targeting, cell uptake and responsive release of siPLK1 in intracellular environment. Tumor penetration capability was further evaluated by single injection of Cy5-labled Ang-NC$_{ss}$(siRNA) into mice bearing orthotopic U87MG tumors, the results indicated that Ang-NC$_{ss}$(siRNA) show a higher distribution in blood vessels and better penetration in glioma as compared to NC$_{ss}$(siRNA), Ang-NC(siRNA), and free siRNA controls (Figure 2i and Figure S4, Supporting Information). With the delivery of Ang-NC$_{ss}$(siRNA), the Cy5-siRNA payload can be transported and detected throughout the whole deep tumor tissue, but little accumulation can be observed in normal brain tissue, indicating the outstanding properties of Ang-NC$_{ss}$(siRNA) for siRNA delivery including highly specific tumor targeting, penetration and efficiently responsive siRNA release.

For pharmacokinetic studies, Cy5-labeled siRNA nanocapsules were administrated with tumor-free mice via tail intravenous (i.v.) and concentrations were measured at different intervals postinjection. Notably, Ang-NC$_{ss}$(siRNA) boosted a long plasma elimination half-life ($t_{1/2, \beta}$) of 46 min, similar to that of NC$_{ss}$(siRNA) and Ang-NC(siRNA). In comparison, naked siRNA was quick eliminated from the circulation and had a short half-life of 5 min (**Figure 3**a), in accordance with reported values.[19] These results verified that Ang peptide does not affect the pharmacokinetics of Ang-NC$_{ss}$(siRNA) nanocapsules. The body distribution of accumulation of siRNA nanocapsules was evaluated in orthotopic U87MG-luc glioblastoma mice model. The siRNA nanocapsules were labeled with Cy5 and monitored

by in vivo near-infrared fluorescence imaging (IVIS Lumia III) after tail i.v. injection. The images displayed that strong Cy5 fluorescence was observed in the brain at 2 h postinjection of Ang-NC$_{ss}$(siRNA), the strong fluorescence intensity sustained up to 24 h (Figure 3b). However, relatively weak fluorescence was observed in glioblastoma of mice with treatment of control groups including NC$_{ss}$(siRNA), Ang-NC(siRNA), and naked siRNA. All these results signifying the critical roles of Ang functionalization and disulfide bond cross-link in the design of Ang-NC$_{ss}$(siRNA) for achieving efficient BBB permeation, glioblastoma accumulation and retention.

To investigate the in vivo gene silencing performance of siRNA nanocapsules, different nanocapsules formulations were injected into mice bearing U87MG-luc orthotopic glioblastoma via a single i.v. administration. In contrast to rapid increase of tumor bioluminescence in mice treated with Ang-NC$_{ss}$(siCtrl), free siGL3 and PBS, the reduction of glioblastoma bioluminescence can be observed in the Ang-NC$_{ss}$(siGL3), NC$_{ss}$(siGL3), and Ang-NC(siGL3) groups (Figure 3c). Furthermore, the quantitative analysis revealed that Ang-NC$_{ss}$(siGL3) resulted in 59% decreasing of tumor bioluminescence, significantly efficient than that of nontargeted NC$_{ss}$(siGL3) (22%) and Ang-NC(siGL3) (20%) at 72 h postsystemic injection (Figure 3d). These results are in line with in vitro gene silencing and further confirm that Ang-NC$_{ss}$(siGL3) can effectively interfere with the expression of the luciferase reporter gene in vitro and in vivo. Interestingly, ex vivo images revealed that mice treated with Ang-NC$_{ss}$(siRNA) had significantly high Cy5-siRNA fluorescence in glioblastoma than other major organs (Figure 3e). Furthermore, Cy5-siRNA fluorescence in glioblastoma treated with Ang-NC$_{ss}$(siRNA) is also stronger than these of NC$_{ss}$(siRNA), Ang-NC(siRNA), and naked siRNA. It should be noted that the Cy5-siRNA fluorescence in brain is well colocalized with the bioluminescence of orthotopic U87MG-luc glioblastoma, indicating the excellent GBM targeting capability of Ang-NC$_{ss}$(siRNA) after passing BBB. The biodistribution of different Cy5-siRNA nanocapsules was also investigated in mice bearing U87MG-luc orthotopic glioblastoma and quantified with fluorometry spectrometer. For Ang-NC$_{ss}$(siRNA), Cy5-siRNA accumulated in tumor was remarkably reach to 6.69% of injected dose per gram of tissue (%ID/g), which was comparable to Ang-NC(siRNA), but 2.7- and 13.6-fold higher than those of NC$_{ss}$(siRNA) and naked siRNA control groups, respectively (Figure 3f). Interestingly, though stronger fluorescence was observed in the tumor than in the liver after 4h post-administration of Ang-NCss(siRNA) (Figure 3e), comparable siRNA accumulation was quantified. This might be ascribed to the encapsulated siRNA being totally extracted and detected by quantification both in tumor and in the liver. Meanwhile, for imaging, the fluorescence of unreleased Cy5-siRNA in liver is readily self-quenched due to the homo fluorescence resonance energy transfer (FRET) effect,[20] which leads to inadequate detection

---

**p < 0.01, ***p < 0.001). g) Western blot assay of Ang-NC$_{ss}$(siPLK1) in U87MG cells following 48 h incubation (400×10^{-9} M siPLK1). h) Apoptosis assay of U87MG cells after 48 h incubation with Ang-NC$_{ss}$(siPLK1) in U87MG cells. i) Tumor penetration behavior of Ang-NC$_{ss}$(siRNA) observed by CLSM. Tumor sections are obtained from U87MG-GBM-bearing mice following 4 h tail vein injection of Ang-NC$_{ss}$(siRNA) (1 mg Cy5-siRNA equiv. kg⁻¹). The nuclei are stained with DAPI (blue) and blood vessels are stained with CD31 (green), Cy5-siRNA are presented as red. Dotted lines indicate the boundary of the tumor. N: normal brain tissue; T: tumor. The scale bars correspond to 50 μm.

**ADVANCED
SCIENCE NEWS**

www.advancedsciencenews.com

**ADVANCED
MATERIALS**

www.advmat.de

Figure 3. a) In vivo pharmacokinetics of Ang-NC$_{ss}$(siRNA), NC$_{ss}$(siRNA), Ang-NC(siRNA), and free siRNA in tumor-free mice (1 mg Cy5-siRNA equiv. kg^{-1}). Cy5-siRNA levels were determined by fluorescence spectroscopy and expressed as injected dose per gram of blood (%ID g^{-1}). Data are presented as mean ± SD ($n = 3$). b) The in vivo fluorescence images of nude mice bearing orthotopic U87MG-luc human glioblastoma tumor at different time points after the injection of Ang-NC$_{ss}$(siRNA), NC$_{ss}$(siRNA), Ang-NC(siRNA), and free siRNA (1 mg Cy5-siRNA equiv. kg^{-1}). c) Luciferase expression of brain in the mice at 0, 24, 48, or 72 h postinjection of Ang-NC$_{ss}$(siGL3), Ang-NC$_{ss}$(siCtrl), NC$_{ss}$(siGL3), Ang-NC(siGL3), or free siGL3 (1 mg siRNA equiv. kg^{-1}). d) Bioluminescence intensity of the glioblastoma tumor. e) Bioluminescence and Cy5-siRNA fluorescence images of major organs from nude mice bearing orthotopic U87MG-luc human glioblastoma tumor 4 h after i.v. injection of Ang-NC$_{ss}$(siRNA), NC$_{ss}$(siRNA), Ang-NC(siRNA), and free siRNA (1 mg Cy5-siRNA equiv. kg^{-1}). f) Quantification of siRNA accumulation in different organs. Cy5-siRNA levels were determined by fluorescence spectroscopy and expressed as injected dose per gram of tissue (%ID g^{-1}). Data are presented as mean ± SD ($n = 3$, one-way ANOVA and Tukey multiple comparisons tests, $*p < 0.05$, $***p < 0.001$).

by the IVIS imaging system. This could also explain though Ang-NC(siRNA) had similar physiochemical properties as compared to Ang-NC$_{ss}$(siRNA), demonstrating quite different imaging results (Figure 3b,e) but similar quantification biodistribution. The antiglioblastoma effect of Ang-NC$_{ss}$(siPLK1) nanocapsules was investigated in U87MG-luc orthotopic xenografts with a totally five-dose injection (siRNA dosage: 2 mg siPLK1 equiv. kg^{-1}). The tumor growth was monitored with an in vivo bioluminescence imaging machine (IVIS Lumia III) by injecting D-luciferin potassium salt substrate. The captured images exhibited that Ang-NC$_{ss}$(siPLK1) potently restrain the

glioblastoma proliferation compared with the NC$_{ss}$(siPLK1) and Ang-NC(siPLK1) controls over the period of the treatment (**Figure 4**a). Unsurprisingly, rapid tumor growth was observed in Ang-NC$_{ss}$(siCtrl), naked siPLK1, and PBS groups. The semiquantitative bioluminescence analysis corroborated that significantly U87MG glioblastoma inhibition was induced by Ang-NC$_{ss}$(siPLK1) nanocapsules versus NC$_{ss}$(siPLK1) and Ang-NC(siPLK1) counterparts (Figure 4b), resulting from effective BBB permeation, enhanced tumor accumulation and retention, selective cellular uptake and responsive siRNA release. Intriguingly, Ang-NC$_{ss}$(siPLK1) caused negligible body weight

ADVANCED
SCIENCE NEWS
www.advancedsciencenews.com

ADVANCED
MATERIALS
www.advmat.de
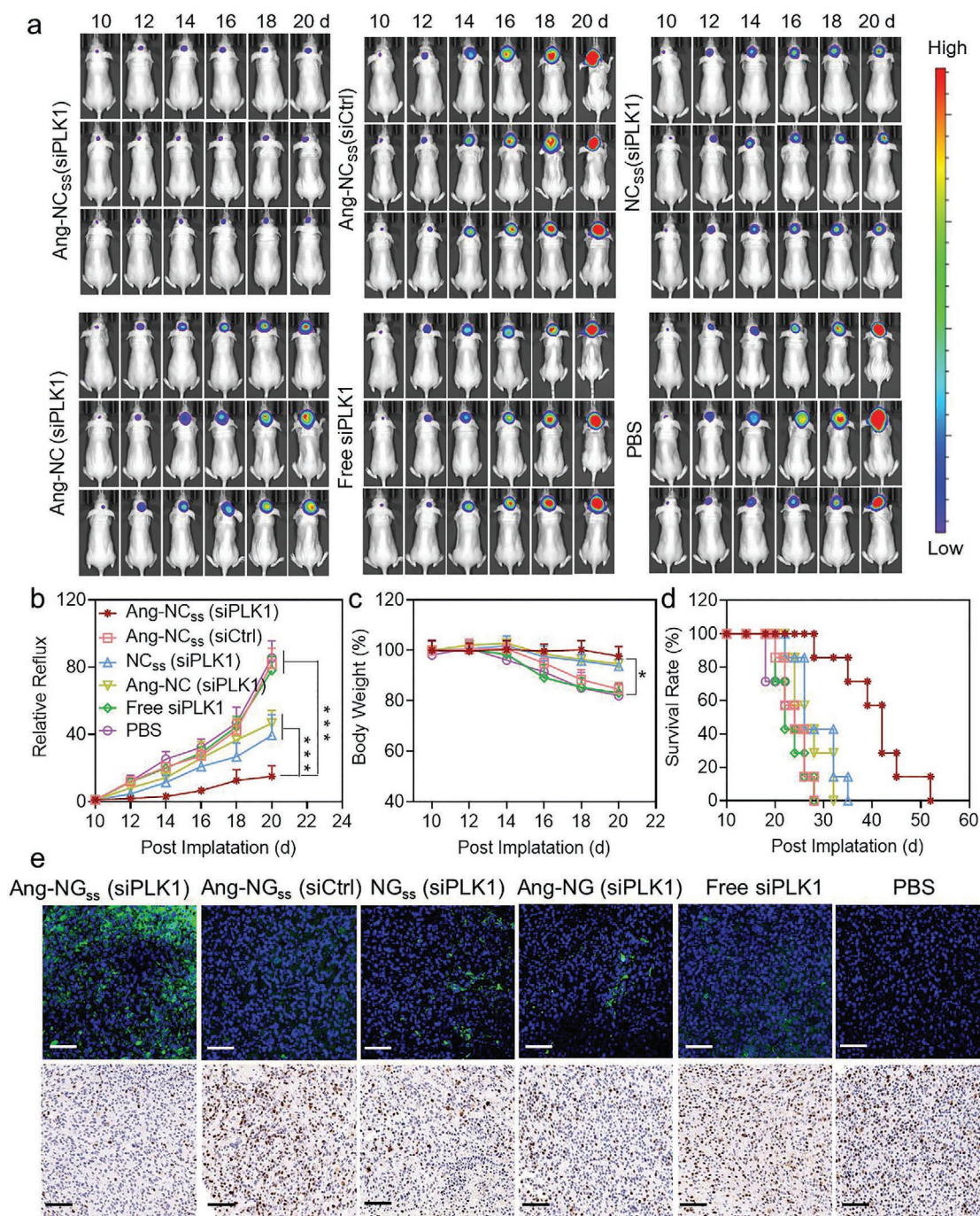
Figure 4. a) Luminescence images of nude mice bearing orthotopic U87MG-luc human glioblastoma tumor after treatment with Ang-NC$_{ss}$(siPLK1), Ang-NC$_{ss}$(siCtrl), NC$_{ss}$(siPLK1), Ang-NC(siPLK1), free siPLK1 or PBS. The mice were intravenously injected at a dose of 2 mg siRNA equiv. kg^{-1} on day 10, 12, 14, 16, and 18 post-tumor implantation. b) Quantified luminescence levels of mice using the Lumina IVIS III system. c) Body weight changes in mice. Data are presented as mean ± SD ($n = 7$, one-way ANOVA and Tukey multiple comparisons tests, *$p < 0.05$, ***$p < 0.001$). d) Mice survival rates. Statistical analysis: Ang-NC$_{ss}$(siPLK1) versus NC$_{ss}$(siPLK1) or Ang-NC(siPLK1), **$p < 0.01$; Ang-NC$_{ss}$(siPLK1) versus Ang-NC$_{ss}$(siCtrl), free siPLK1 or PBS, ***$p < 0.001$ (Kaplan–Meier analysis, log-rank test). e) Tumor slices excised from nude mice bearing orthotopic U87MG-luc human glioblastoma tumor following treatment using TUNEL and proliferation (Ki67) staining. Scale bars were 100 µm for TUNEL and 200 µm for Ki67, respectively.

change, indicating that they can efficiently inhibit the growth of glioblastoma without adverse effects (Figure 4c). In comparison, mice with treatment of Ang-NC$_{ss}$(siCtrl), free siPLK1 and PBS revealed significantly body weight loss (≈30%) in 20 d,

likely due to the fast glioblastoma progression and aggressive invasion into the healthy central nervous system in the brain of treated mice model. Kaplan–Meier survival curves showed that mice treated with Ang-NC$_{ss}$(siPLK1) significantly expanded the

survival time of glioblastoma-bearing mice, which had a long median survival time of 42 d (Figure 4d). Meanwhile, animals treated with Ang-NC$_{ss}$(siCtrl), free siPLK1, and PBS all died in 28 d. The nontargeted NC$_{ss}$(siPLK1) and nonreduction Ang-NC(siPLK1) groups partially improved the mice survival rate, in which median survival time of 26 d. Notably, reduction PLK1 mRNA in tumors was detected for Ang-NC$_{ss}$(siPLK1) nanocapsules treatments (Figure S5, Supporting Information).

To unveil the apoptosis induction of these nanocapsules, in situ TUNEL assay was employed for glioblastoma tissue analysis after treatment with different groups. The glioblastoma tissue collected from Ang-NC$_{ss}$(siPLK1) showed the highest apoptosis level in the tumor among all the groups. Moreover, the immunohistochemistry analysis of proliferation further indicated these nanocapsules induced the lowest level of tumor cell proliferation (Figure 4e). Histological analysis using H&E staining demonstrated that all nanocapsules have negligible damage to the major organs (Figure S6, Supporting Information). We further performed serial daily blood monitoring of white blood cell (WBC), red blood cell (RBC), and platelet (PLT) levels in healthy Balb/C mice. The results shows that mice treated with Ang-NC$_{ss}$(siPLK1) had considerably stable WBC, RBC and PLT levels over the treatment course compared to PBS groups (Figure S7a–c, Supporting Information). Furthermore, the body weight of mice treated with Ang-NC$_{ss}$(siPLK1) had minimal change during the period (Figure S7d, Supporting Information). These data suggest that Ang-NC$_{ss}$(siPLK1) possess good biocompatibility. We have successfully developed a novel strategy for effective brain siRNA delivery that self-encapsulates therapeutic siRNA within an intracellular environment responsive polymeric shell to produce ultrasmall siRNA nanocapsules, followed by functionalized with a simple targeting ligand which can target both BBB-transport and tumor cells in the brain using a "one stone two birds" strategy. The developed brain targeting siRNA nanocapsules (Ang-NC$_{ss}$(siRNA)) uniquely integrate all functions in one: i) they have a particular small size with a polymeric shell which can protect siRNA in core from degradation during the multi-step delivery process and facilitate BBB penetration; ii) they are stable in plasma and have a long siRNA circulation time; iii) they can not only effectively cross BBB via LRP-1 mediated transcytosis mechanism but selectively internalized by U87MG glioblastoma cells via LRP-1 receptor mediated endocytosis (one stone two birds); iv) they responsively release siRNA into the cytoplasmic due to GSH triggered nanocapsule degradation, leading to efficacious and specific gene knockdown; v) in addition to high RNAi and tumor inhibition efficacy, they are safe and easy to be fabricated with a high yield of siRNA encapsulation. We believe developed siRNA capsules with these superior advantages not only offer a safe and efficient tool for glioblastoma RNAi therapy, but also can be used in other brain disease therapy.

Supporting Information

Supporting Information is available from the Wiley Online Library or from the author.

[1] a) B. M. Alexander, T. F. Cloughesy, *J. Clin. Oncol.* **2017**, *35*, 2402; b) K. Aldape, G. Zadeh, S. Mansouri, G. Reifenberger, A. von Deimling, *Acta Neuropathol.* **2015**, *129*, 829.

[2] a) M. Lim, Y. Xia, C. Bettegowda, M. Weller, *Nat. Rev. Clin. Oncol.* **2018**, *15*, 422; b) J. Wang, E. Cazzato, E. Ladewig, V. Frattini, D. I. S. Rosenbloom, S. Zairis, F. Abate, Z. Liu, O. Elliott, Y.-J. Shin, J.-K. Lee, I.-H. Lee, W.-Y. Park, M. Eoli, A. J. Blumberg, A. Lasorella, D.-H. Nam, G. Finocchiaro, A. Iavarone, R. Rabadan, *Nat. Genet.* **2016**, *48*, 768.

[3] a) M. Mehta, P. Wen, R. Nishikawa, D. Reardon, K. Peters, *Crit. Rev. Oncol./Hematol.* **2017**, *111*, 60; b) A. Desjardins, M. Gromeier, J. E. Herndon, N. Beaubier, D. P. Bolognesi, A. H. Friedman, H. S. Friedman, F. McSherry, A. M. Muscat, S. Nair, K. B. Peters, D. Randazzo, J. H. Sampson, G. Vlahovic, W. T. Harrison, R. E. McLendon, D. Ashley, D. D. Bigner, *N. Engl. J. Med.* **2018**, *379*, 150.

[4] P. D. Delgado-López, E. M. Corrales-García, *Clin. Transl. Oncol.* **2016**, *18*, 1062.

[5] a) J.-L. Huang, G. Jiang, Q.-X. Song, X. Gu, M. Hu, X.-L. Wang, H.-H. Song, L.-P. Chen, Y.-Y. Lin, D. Jiang, J. Chen, J.-F. Feng, Y.-M. Qiu, J.-Y. Jiang, X.-G. Jiang, H.-Z. Chen, X.-L. Gao, *Nat. Commun.* **2017**, *8*, 15144; b) S. An, D. He, E. Wagner, C. Jiang, *Small* **2015**, *11*, 5142; c) Y. Jiang, R. Tang, B. Duncan, Z. Jiang, B. Yan, R. Mout, V. M. Rotello, *Angew. Chem., Int. Ed.* **2015**, *54*, 506; d) M. Yan, M. Liang, J. Wen, Y. Liu, Y. Lu, I. S. Y. Chen, *J. Am. Chem. Soc.* **2012**, *134*, 13542.

[6] a) D. Rosenblum, N. Joshi, W. Tao, J. M. Karp, D. Peer, *Nat. Commun.* **2018**, *9*, 1410; b) W. Tai, J. Li, E. Corey, X. Gao, *Nat. Biomed. Eng.* **2018**, *2*, 326.

[7] a) D. Wang, P. W. L. Tai, G. Gao, *Nat. Rev. Drug Discovery* **2019**, *18*, 358; b) H. Yin, K. J. Kauffman, D. G. Anderson, *Nat. Rev. Drug Discovery* **2017**, *16*, 387; c) R. Ni, J. Zhou, N. Hossain, Y. Chau, *Adv. Drug Delivery Rev.* **2016**, *106*, 3.

[8] a) B. Kim, J.-H. Park, M. J. Sailor, *Adv. Mater.* **2019**, *31*, 1903637; b) W. Viricel, A. Mbarek, J. Leblond, *Angew. Chem., Int. Ed.* **2015**, *54*,

12743; c) R. L. Ball, K. A. Hajj, J. Vizelman, P. Bajaj, K. A. Whitehead, *Nano Lett.* **2018**, *18*, 3814.

[9] a) O. F. Khan, P. S. Kowalski, J. C. Doloff, J. K. Tsosie, V. Bakthavatchalu, C. B. Winn, J. Haupt, M. Jamiel, R. Langer, D. G. Anderson, *Sci. Adv.* **2018**, *4*, eaar8409; b) J. M. Priegue, D. N. Crisan, J. Martínez-Costas, J. R. Granja, F. Fernandez-Trillo, J. Montenegro, *Angew. Chem., Int. Ed.* **2016**, *55*, 7492.

[10] a) A. Kohata, P. K. Hashim, K. Okuro, T. Aida, *J. Am. Chem. Soc.* **2019**, *141*, 2862; b) D.-H. Park, J. Cho, O.-J. Kwon, C.-O. Yun, J.-H. Choy, *Angew. Chem., Int. Ed.* **2016**, *55*, 4582.

[11] a) C.-Y. Sun, S. Shen, C.-F. Xu, H.-J. Li, Y. Liu, Z.-T. Cao, X.-Z. Yang, J.-X. Xia, J. Wang, *J. Am. Chem. Soc.* **2015**, *137*, 15217; b) X. Xu, J. Wu, Y. Liu, P. E. Saw, W. Tao, M. Yu, H. Zope, M. Si, A. Victorious, J. Rasmussen, D. Ayyash, O. C. Farokhzad, J. Shi, *ACS Nano* **2017**, *11*, 2618; c) M. A. Rahman, P. Wang, Z. Zhao, D. Wang, S. Nannapaneni, C. Zhang, Z. Chen, C. C. Griffith, S. J. Hurwitz, Z. G. Chen, Y. Ke, D. M. Shin, *Angew. Chem., Int. Ed.* **2017**, *56*, 16023.

[12] a) M. Zheng, W. Tao, Y. Zou, O. C. Farokhzad, B. Shi, *Trends Biotechnol.* **2018**, *36*, 562; b) Y. Wang, L. Huang, *Nat. Biotechnol.* **2013**, *31*, 611; c) H. J. Kim, A. Kim, K. Miyata, K. Kataoka, *Adv. Drug Delivery Rev.* **2016**, *104*, 61.

[13] a) Y. Zou, Y. Liu, Z. Yang, D. Zhang, Y. Lu, M. Zheng, X. Xue, J. Geng, R. Chung, B. Shi, *Adv. Mater.* **2018**, *30*, 1803717; b) Y. Jiang, W. Yang, J. Zhang, F. Meng, Z. Zhong, *Adv. Mater.* **2018**, *30*, 1800316; c) Y. Jiang, J. Zhang, F. Meng, Z. Zhong, *ACS Nano* **2018**, *12*, 11070.

[14] a) X. Guo, L. Wang, K. Duval, J. Fan, S. Zhou, Z. Chen, *Adv. Mater.* **2018**, *30*, 1705436; b) D. Li, N. Kordalivand, M. F. Fransen, F. Ossendorp, K. Raemdonck, T. Vermonden, W. E. Hennink, C. F. van Nostrum, *Adv. Funct. Mater.* **2015**, *25*, 2993; c) X. Hu, S. Zhai, G. Liu, D. Xing, H. Liang, S. Liu, *Adv. Mater.* **2018**, *30*, 1706307.

[15] M. Yan, J. Du, Z. Gu, M. Liang, Y. Hu, W. Zhang, S. Priceman, L. Wu, Z. H. Zhou, Z. Liu, T. Segura, Y. Tang, Y. Lu, *Nat. Nanotechnol.* **2010**, *5*, 48.

[16] M. Zheng, Y. Liu, Y. Wang, D. Zhang, Y. Zou, W. Ruan, J. Yin, W. Tao, J. B. Park, B. Shi, *Adv. Mater.* **2019**, *31*, 1903277.

[17] M. Li, Z. Luo, Z. Xia, X. Shen, K. Cai, *Mater. Horiz.* **2017**, *4*, 977.

[18] X. Xu, J. Wu, Y. Liu, P. Saw, W. Tao, M. Yu, H. Zope, M. Si, A. Victorious, J. Rasmussen, D. Ayyash, O. C. Farokhzad, J. Shi, *ACS Nano* **2017**, *11*, 2618.

[19] a) Y.-d. Yao, T.-m. Sun, S.-y. Huang, S. Dou, L. Lin, J.-n. Chen, J.-b. Ruan, C.-q. Mao, F.-y. Yu, M.-s. Zeng, J.-y. Zang, Q. Liu, F.-x. Su, P. Zhang, J. Lieberman, J. Wang, E. Song, *Sci. Transl. Med.* **2012**, *4*, 130ra48; b) S. M. Sarett, T. A. Werfel, L. Lee, M. A. Jackson, K. V. Kilchrist, D. Brantley-Sieders, C. L. Duvall, *Proc. Natl. Acad. Sci. USA* **2017**, *114*, E6490.

[20] a) Y. Wang, C. Wang, Y. Li, G. Huang, T. Zhao, X. Ma, Z. Wang, B. D. Sumer, M. A. White, J. Gao, *Adv. Mater.* **2017**, *29*, 1603794; b) R. Lizatović, M. Assent, A. Barendregt, J. Dahlin, A. Bille, K. Satzinger, D. Tupina, A. J. R. Heck, S. Wennmalm, I. André, *Angew. Chem.* **2018**, *130*, 11504.